

On the Multi-Layered Adsorption of Alkanols in the Vicinity of Liquid–Vapor Transition at the Saturated Hydrocarbon/Water Interface

A. M. Tikhonov^{a,*} and Yu. O. Volkov^{b,**}

^a Kapitza Institute for Physical Problems, Russian Academy of Sciences, Moscow, 119334 Russia

^b National Research Center “Kurchatov Institute”, Moscow, 123182 Russia

*e-mail: tikhonov@kapitza.ras.ru

**e-mail: volkov.y@crys.ras.ru

Received October 28, 2023; revised January 12, 2024; accepted January 12, 2024

Abstract—Structure of the adsorption layer of unsaturated monoatomic alcohols, 1-dodecanol and 1-tetracosanol, at *n*-hexane/water and *n*-hexadecane/water interfaces, respectively, in the vicinity of liquid–vapor thermotropic phase transition is investigated by the method of X-ray reflectometry with a synchrotron source. Model-independent structural data obtained on the adsorption layers under investigation deviate considerably from the structural parameters that have been previously proposed within a model-based approach and discussed for the said systems. It is shown that in the low-temperature mesophase the adsorption film consists of a Gibbs monolayer, a liquid transition region with thickness of two to three monolayers ~ 50 Å, and an extended (wide up to 200 Å) layer of micelles. Presence of a plane of the closest approach of the micellar layer to the adsorption film at the interface is established. Transition to the high-temperature mesophase is accompanied by liquefying and partial evaporation of the alkanol film along with depletion of the micellar layer down to its complete disappearance.

Keywords: X-ray reflectometry, liquid interfaces

DOI: 10.1134/S1027451024700010

INTRODUCTION

A soluble adsorption film at the liquid/liquid interface can be considered a two-dimensional thermodynamic system with parameters (p , T , c), where p is pressure, T is temperature, and c is concentration of surface-active impurities in the bulk of solvent [1]. An example of such a system is a layer of saturated monoatomic alcohol (alkanol) at the saturated hydrocarbon/water interface [2, 3]. In a film of a long-chain alkanol dissolved in a hydrocarbon, a phase transition is possible, which can be of thermotropic, barotropic, or lyotropic nature [4, 5]. For example, thermotropic transition ($p = 1$ atm and $c = \text{const}$) can manifest itself either as a sharp change in the surface state or as a prolonged temperature change accompanied by the formation of a spatially inhomogeneous surface structure [6, 7]. Moreover, thermotropic liquid–vapor phase transformations are observed in layers of *n*-alkanols [8], and a solid–gas transition occurs in films of fluoroalkanols [9]. Similar phenomena were also observed in two-component adsorption films [10].

At the phase transition point T_c in a film of long-chain alkanol, a feature (kink) is observed on the tem-

perature dependence of interfacial tension $\gamma(T)$, which can be associated with the change in enthalpy $\Delta H = -T_c \Delta(\partial\gamma/\partial T)_{p,c}$ when the film evaporates. Note that ΔH strongly depends on ratio $r = m/m_0$ of the number of carbon atoms in alkanol m to the number of carbon atoms in the solvent molecule m_0 [11]. For example, for $C_{12}OH$ at the *n*-hexane/water interface the value of ΔH is 10 times less than that for $C_{30}OH$ at the same interface. Increasing the length of the solvent molecule from six to sixteen carbon atoms also greatly reduces ΔH for alkanols $C_{24}OH$ and $C_{30}OH$. Note that, according to detailed studies, the value of ΔH is practically independent of volume concentration c , for example, during a lyotropic transition in a film of arachidyl alcohol ($C_{20}OH$) at the *n*-hexane/water interface [12].

The main distinctive feature of *n*-dodecanol ($C_{12}OH$) and *n*-tetracosanol ($C_{24}OH$) films at planar interfaces *n*-hexane/water and *n*-hexadecane/water, respectively, is a relatively low value of the enthalpy of thermotropic transition. Previously, the transition of complete wetting of the surface of an aqueous substrate with an alkanol film was discussed for these sys-

tems using data from multiparameter models [11]. In particular, there were qualitative differences in the adsorption of long-chain alkanols ($C_{24}OH$ and $C_{30}OH$) depending on the transition enthalpy. However, attempts to describe some adsorption systems within the framework of models led to significantly ambiguous (including mutually contradictory) interpretations of their structure.

In this work, the structural parameters of multilayer adsorption films of dodecanol and tetracosanol near the thermotropic transition temperature are refined using experimental X-ray reflectometry data with synchrotron radiation in the framework of a model-independent reconstruction that makes it possible to unambiguously extract the electron concentration distribution in the studied samples.

EXPERIMENTAL

Samples of alkanol/water interfacial systems were prepared and studied under normal conditions in a thermostated cell according to the method described in [13]. Solutions of 1-dodecanol $C_{12}H_{25}OH$ in *n*-hexane C_6H_{14} (density $\rho_t \approx 0.655 \text{ g/cm}^3$ at $T = 20^\circ\text{C}$, boiling point $T_b = 68^\circ\text{C}$) with a volume concentration of $\sim 45 \text{ mmol/L}$ and 1-tetracosanol $C_{24}H_{49}OH$ in *n*-hexadecane $C_{16}H_{34}$ (density $\rho_t \approx 0.773 \text{ g/cm}^3$ at $T = 20^\circ\text{C}$, boiling point $T_b = 286.7^\circ\text{C}$) with a volume concentration of $\sim 4 \text{ mmol/L}$ (Sigma-Aldrich) were used as the upper oil phase. Deionized water $\text{pH} \approx 7$ (NanoPureUV) was used as the lower phase. Before preparing the sample, the liquids were degassed in an ultrasonic bath. As the temperature increased during measurements, the samples were brought into equilibrium for several hours under gentle mechanical stirring of the lower phase.

Angular dependences of the specular reflection coefficient of radiation $R(q_z)$ (where $q_z = (4\pi/\lambda)\sin\alpha$) were measured on the X19C station of an NSLS synchrotron [14]. Probing monochromatic beam with energy $E = 15 \text{ keV}$ ($\lambda = 0.825 \pm 0.002 \text{ \AA}$) and angular divergence $< 10^{-5}$ rad provided intensity $\sim 10^{11}$ photons/s. Experimental reflection curves from the *n*-hexane/water interface obtained at temperatures of 8.0, 20.0, and 55.1°C are shown in Fig. 1; the reflection curves from the *n*-hexadecane/water interface obtained at temperatures of 50.8, 53.0, and 81.9°C are shown in Fig. 2.

Reconstruction of volumetric electron density distributions over depth $\rho(z)$ from experimental curves was carried out using a model-independent approach [15, 16]. The calculations were implemented in the Python language using the Scientific Python and PyLab library packages. Reconstructed distributions

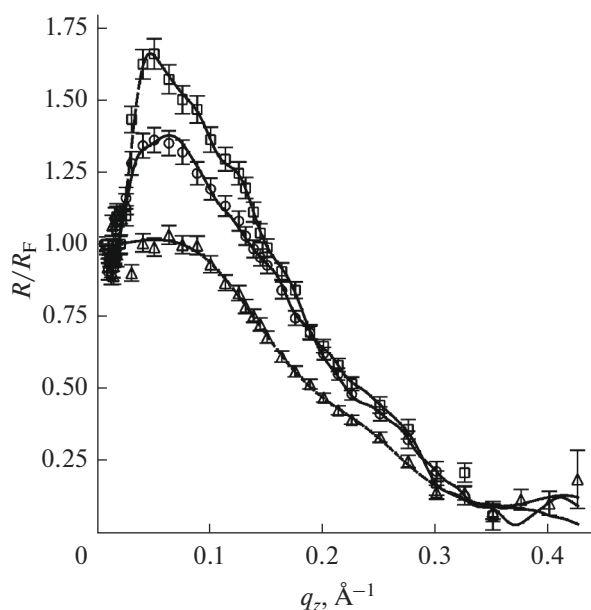


Fig. 1. Angular dependences of the reflection coefficient R from dodecanol at the *n*-hexane/water interface normalized to the Fresnel function R_F in low-temperature ($T = 8.0^\circ\text{C}$, circles; $T = 20.0^\circ\text{C}$, squares) and high-temperature ($T = 55.1^\circ\text{C}$, triangles) phases. The lines indicate the calculated reflection curves.

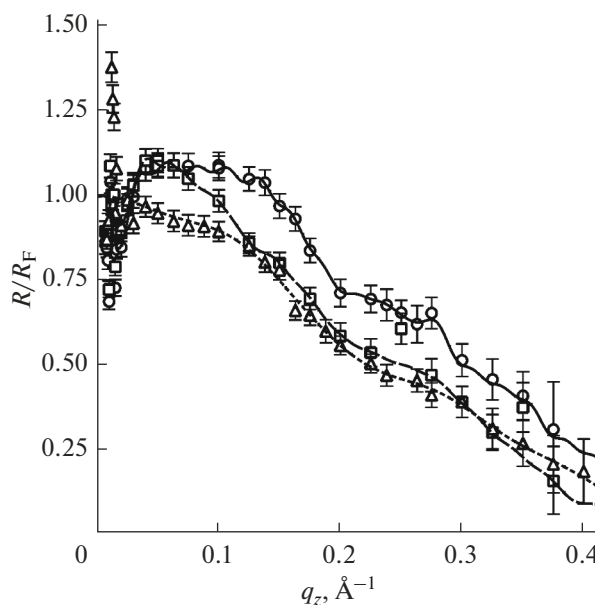


Fig. 2. Angular dependences of the reflection coefficient R from tetracosanol at the *n*-hexadecane/water interface normalized to the Fresnel function R_F in low-temperature ($T = 50.8^\circ\text{C}$, circles), transition ($T = 53.0^\circ\text{C}$, squares), and high-temperature ($T = 81.9^\circ\text{C}$, triangles) phases. The lines indicate the calculated reflection curves.

$\rho(z)$ at the *n*-hexane/water interface and the *n*-hexadecane/water interface are presented in Figs. 3 and 4, respectively.

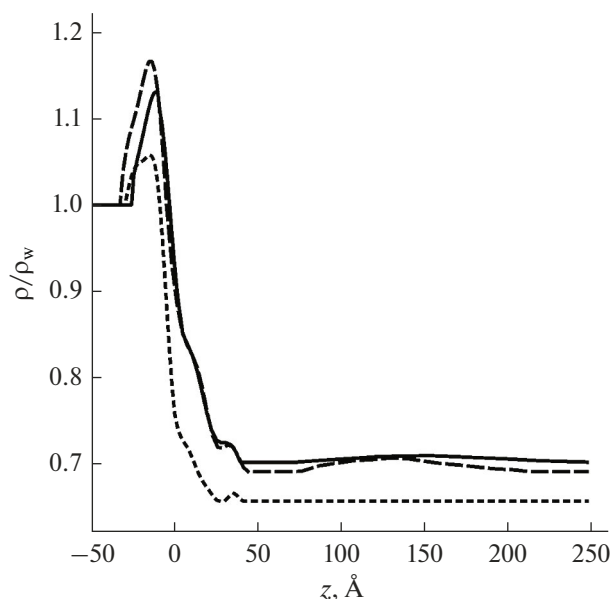


Fig. 3. Reconstructed electron density profiles $\rho(z)$ for the *n*-hexane/water interface normalized to the electron concentration in water under normal conditions $\rho_w = 0.333 \text{ e}/\text{\AA}^3$ in low-temperature ($T = 8.0^\circ\text{C}$, solid line; $T = 20.0^\circ\text{C}$, dashed line) and high-temperature ($T = 55.1^\circ\text{C}$, dotted line) phases.

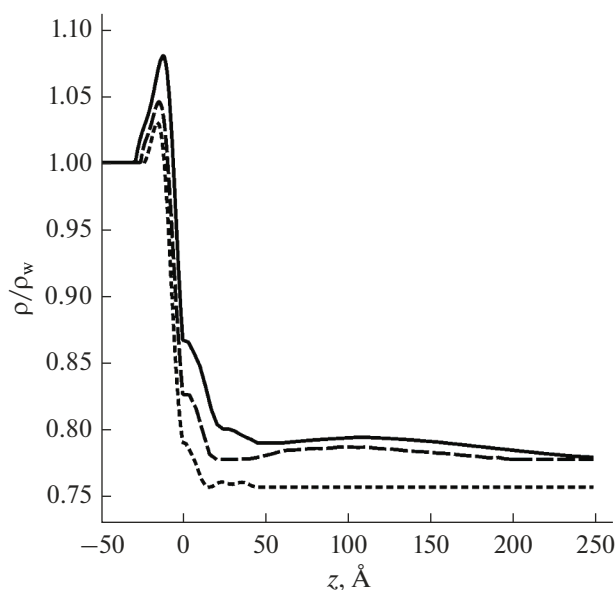


Fig. 4. Reconstructed electron density profiles $\rho(z)$ for the *n*-hexadecane/water interface normalized to the electron concentration in water under normal conditions $\rho_w = 0.333 \text{ e}/\text{\AA}^3$ in low-temperature ($T = 50.8^\circ\text{C}$, solid line), transition ($T = 53.0^\circ\text{C}$, dashed line), and high-temperature ($T = 81.9^\circ\text{C}$, dotted line) phases.

RESULTS AND DISCUSSION

To a first approximation, the adsorbed layer at the alkane/water interface is a Gibbs monolayer of alcohol

molecules. Total length of alkanol molecules L_{trans} is determined by the length of the carbon chain (based on $\approx 1.3 \text{ \AA}$ per C–C bond) and the sizes of the methyl $-\text{CH}_3$ ($\approx 1.5 \text{ \AA}$) and hydroxyl $-\text{CH}_2\text{OH}$ ($\approx 2.4 \text{ \AA}$) groups. Thus, L_{trans} varies from $\approx 17 \text{ \AA}$ (for $m = 12$, 1-dodecanol) to $\approx 32 \text{ \AA}$ (for $m = 24$, 1-tetracosanol). At room temperature the hydrocarbon chains of alcohols undergo conformational isomerization so that the actual length of the monomers in solution is shorter than L_{trans} .

According to [8], for 1-dodecanol at the *n*-hexane/water interface the critical evaporation temperature is $T_c \approx 37^\circ\text{C}$ and for 1-tetracosanol at the *n*-hexadecane/water interface $T_c \approx 62^\circ\text{C}$. For systems of both studied alkanols in the low-temperature phase ($T < T_c$, solid lines in Figs. 3, 4) we observed a multilayer structure with a total thickness of up to $\sim 75 \text{ \AA}$, including at least three molecular layers with a density that decreases with distance from the water surface, as well as a loose layer in the bulk of the solvent near the interface with a thickness of up to $\sim 200 \text{ \AA}$. It is known that in the triad “nonpolar solvent–amphiphilic surfactant–water,” when the critical concentration of surfactant is exceeded ($>1 \text{ mmol/L}$) in an oil solution, micelles are formed that are in thermodynamic equilibrium with monomers [17, 18]. Note that in both systems there is a plane of closest approach ($\sim 25 \text{ \AA}$) between the micellar layer and the surface film, which is presumably due to electrostatic effects at the interface.

Integral characteristic of a dense molecular monolayer of surfactant is the specific area per molecule $A = (1/M) \int_L \rho(z) dz$, where M is the number of electrons in an alcohol molecule ($M = 106$ for dodecanol and 214 for tetracosanol). Integration was carried out over the thickness of the monolayer $L \sim L_{\text{trans}}$. In the case of the low temperature phase, the estimated value of A was 20 ± 1 and $23 \pm 1 \text{ \AA}^2$ for C_{12} - and C_{24} -alkanol, respectively, which is close to the values for a bulk crystal. At the same time, in the transition region between the dense monolayer and adsorbed micelles, the bulk density is 1.35–1.40 times lower compared to the monolayer, which approximately corresponds to an alkane liquid or, possibly, a mixture of alkanol and solvent molecules.

In turn, in the high-temperature phase ($T > T_c$, dotted lines in Figs. 3, 4), the micellar layer in the bulk of the solvent disappears, and the density of the adsorption film decreases by $(\rho_1 - \rho_b)/(\rho_2 - \rho_b) \approx 1.2$ times (where ρ_b is the bulk electron density of the oil phase and ρ_1 and ρ_2 are the Gibbs monolayer densities in the low-temperature and high-temperature mesophases of the film, respectively) for both

alkanols, which corresponds to the melting of the monolayer and, moreover, partial evaporation of alcohol molecules from the interface.

The adsorption of surfactant molecules at the saturated hydrocarbon/water interface can be considered within the framework of the mechanism of adsorption of a single-component gas onto a solid substrate. In particular, the adsorption of a gas onto a substrate at a fixed temperature will increase with increasing pressure (or chemical potential), bringing the system closer to the liquid/gas interface in the phase diagram. In the *n*-hexane–water system, the analog of the gas is the alkanol molecules and the analog of the solid substrate is the water surface. With a change in the length of the alkane solvent molecule, the effective interaction between alkanol molecules changes from gas-like (when the alkane molecule is much shorter than the alkanol molecule) to liquid-like (when the alkane molecule is almost equal to the length of the alkanol molecule).

Due to a small enthalpy of thermotropic transition for film C₁₂OH ($\Delta H \approx 0.05$ mJ/m²) it should be expected that there is a fairly wide transition temperature range ΔT_c , in which a spatially inhomogeneous structure is formed from domains of low- and high-temperature phases. For example, for a film of 1,1,2,2-tetrahydroheptadecafluorodecanol ($\Delta H \approx 0.15$ mJ/m²) the observed width of the transition region is > 10 K [19], while for film C₂₂OH with a relatively large $\Delta H \approx 0.7$ mJ/m² interval $\Delta T_c < 0.01$ K [7]. Perhaps for this reason, in the C₁₂OH film the gas phase is not realized in pure form up to the boiling point of *n*-hexane at $T \approx 68^\circ\text{C}$. However, it actually exhibits a low-contrast structure, in which the packing density of the hydrocarbon tails of 1-dodecanol is $\approx 0.7\rho_w$, which is noticeably lower than the electron concentration in a high-molecular alkane liquid ($\approx 0.85\rho_w$). Refinement of the domain structure of the observed structure will require, for example, the use of grazing nonspecular scattering data.

Note that a change in the adsorption mechanism can lead to the transition of complete wetting of the water surface (substrate) by layers of alkanol (gas) [20]. However, for a more detailed study of the issue of transition to complete wetting, in our opinion, it is necessary to study adsorption in a wider range of alkane–alkanol–water systems.

FUNDING

The work was carried out within the framework of State Assignments for the Kapitza Institute for Physical Prob-

lems, Russian Academy of Sciences and the National Research Center “Kurchatov Institute.”

CONFLICT OF INTEREST

The authors of this work declare that they have no conflicts of interest.

REFERENCES

1. J. W. Gibbs, *Collected Works* (Dover, New York, 1961), Vol. 1, p. 219.
2. J. J. Jasper and B. L. Houseman, *J. Phys. Chem.* **67**, 1548 (1963).
<https://www.doi.org/10.1021/j100801a035>
3. K. Motomura, *J. Colloid Interface Sci.* **64**, 348 (1978).
[https://www.doi.org/10.1016/0021-9797\(78\)90372-7](https://www.doi.org/10.1016/0021-9797(78)90372-7)
4. M. Lin, J. L. Ferpo, P. Mansaura, and J. F. Baret, *J. Chem. Phys.* **71**, 2202 (1979).
<https://www.doi.org/10.1063/1.438551>
5. Y. Hayami, A. Uemura, M. Ikeda, M. Aratono, and K. Motomura, *J. Colloid Interface Sci.* **172** 142 (1995).
<https://www.doi.org/10.1006/jcis.1999.6536>
6. S. Uredat and G. H. Findenegg, *Langmuir* **15**, 1108 (1999). <https://www.doi.org/10.1021/la981264q>
7. M. Aratono, D. Murakami, H. Matsubara, and T. Takiue, *J. Phys. Chem. B* **113**, 6347 (2009).
<https://www.doi.org/10.1021/jp9001803>
8. A. M. Tikhonov, S. V. Pingali, and M. L. Schlossman, *J. Chem. Phys.* **120**, 11822 (2004).
<https://www.doi.org/10.1063/1.1752888>
9. Z. Zhang, D. M. Mitrinovic, S. M. Williams, Z. Huang, and M. L. Schlossman, *J. Chem. Phys.* **110**, 7421 (1999).
<https://www.doi.org/10.1063/1.478644>
10. S. V. Pingali, T. Takiue, L. Guangming, A. M. Tikhonov, N. Ikeda, M. Aratono, and M. L. Schlossman, *J. Dispersion Sci. Technol.* **27**, 715 (2006).
<https://www.doi.org/10.1080/01932690600660582>
11. A. M. Tikhonov and M. L. Schlossman, *J. Phys.: Condens. Matter* **19**, 375101 (2007).
<https://www.doi.org/10.1088/0953-8984/19/37/375101>
12. T. Takiue, T. Matsuo, N. Ikeda, K. Motomura, and M. Aratono, *J. Phys. Chem. B* **102**, 4906 (1998).
<https://www.doi.org/10.1021/jp980292e>
13. A. M. Tikhonov, V. E. Asadchikov, Yu. O. Volkov, A. D. Nuzhdin, and B. S. Roshchin, *Prib. Tekh. Eksp.*, No. 1, 146 (2021).
<https://www.doi.org/10.31857/S0032816221010158>
14. M. L. Schlossman, D. Synal, Y. Guan, M. Meron, G. Shea-McCarthy, Z. Huang, A. Acero, S. M. Williams, S. A. Rice, and P. J. Viccaro, *Rev. Sci. Instrum.* **68**, 4372 (1997).
<https://www.doi.org/10.1063/1.1148399>

15. I. V. Kozhevnikov, Nucl. Instrum. Methods Phys. Res. A **508**, 519 (2003).
[https://www.doi.org/10.1016/S0168-9002\(03\)01512-2](https://www.doi.org/10.1016/S0168-9002(03)01512-2)
16. I. V. Kozhevnikov, L. Peverini, and E. Ziegler, Phys. Rev. B **85**, 125439 (2012).
<https://doi.org/10.1103/PhysRevB.85.125439>
17. P. Becher, *Emulsions: Theory and Practice* (Oxford Univ. Press, Oxford, 2001).
18. G. N. Smith, P. Brown, S. E. Rogers, and J. Eastoe, Langmuir **29**, 3252 (2013).
<https://www.doi.org/10.1021/la400117s>
19. A. M. Tikhonov, M. Li, and M. L. Schlossman, J. Phys. Chem. B **105**, 8065 (2001).
<https://doi.org/10.1021/jp011657p>
20. E. Bertrand, H. Dobbs, D. Broseta, J. Indekeu, D. Bonn, and J. Meunier, Phys. Rev. Lett. **85**, 1282 (2000).
<https://www.doi.org/10.1103/PhysRevLett.85.1282>

Publisher's Note. Pleiades Publishing remains neutral with regard to jurisdictional claims in published maps and institutional affiliations.